An apoA-I mimetic peptibody generates HDL-like particles and increases alpha-1 HDL subfraction in mice[S]

Shu-Chen Lu,[1,*] Larissa Atangan,[*] Ki Won Kim,[*] Michelle M. Chen,[*] Renee Komorowski,[*] Carolyn Chu,[†] Joon Han,[†] Sylvia Hu,[†] Wei Gu,[*] Murielle Véniant,[*] and Minghan Wang[*]

Departments of Metabolic Disorders,[*] and Protein Sciences,[†] Amgen, Inc., Thousand Oaks, CA 91320

Abstract **The aim of this study is to investigate the capability of an apoA-I mimetic with multiple amphipathic helices to form HDL-like particles in vitro and in vivo. To generate multivalent helices and to track the peptide mimetic, we have constructed a peptibody by fusing two tandem repeats of 4F peptide to the C terminus of a murine IgG Fc fragment. The resultant peptidbody, mFc-2X4F, dose-dependently promoted cholesterol efflux in vitro, and the efflux potency was superior to monomeric 4F peptide. Like apoA-I, mFc-2X4F stabilized ABCA1 in J774A.1 and THP1 cells. The peptibody formed larger HDL particles when incubated with cultured cells compared with those by apoA-I. Interestingly, when administered to mice, mFc-2X4F increased both pre-β and α-1 HDL subfractions. The lipid-bound mFc-2X4F was mostly in the α-1 migrating subfraction. Most importantly, mFc-2X4F and apoA-I were found to coexist in the same HDL particles formed in vivo.[F1] These data suggest that the apoA-I mimetic peptibody is capable of mimicking apoA-I to generate HDL particles. The peptibody and apoA-I may work cooperatively to generate larger HDL particles in vivo, either at the cholesterol efflux stage and/or via fusion of HDL particles that were generated by the peptibody and apoA-I individually.**—Lu, S-C., L. Atangan, K. Won Kim, M. M. Chen, R. Komorowski, C. Chu, J. Han, S. Hu, W. Gu, M. Véniant, and M. Wang. **An apoA-I mimetic peptibody generates HDL-like particles and increases alpha-1 HDL subfraction in mice. *J. Lipid Res.* 2012.** 53: **643–652.**

Supplementary key words apolipoprotein AI • atherosclerosis • ATP binding cassette transporter A1 • cholesterol efflux • 4F peptide • high density lipoprotein

HDL has been identified as a potential target for the treatment of atherosclerotic vascular disease. Nascent HDL is formed by the interaction of apoA-I and ABCA1, which triggers the cholesterol and phospholipid efflux from cells, the first step of reverse cholesterol transport (1, 2). ApoA-I has also been shown in animal models and humans to have the therapeutic potential of reversing atherosclerosis (3–5). ApoA-I is a 243 amino acid protein with amphipathic α-helices (6). This amphipathic structure is considered to be important for its biological function in cholesterol efflux (7, 8). Recently, several small amphipathic peptides including 18A, 37pA, and 4F have been reported (9, 10). Although these apoA-I mimetics have been shown to promote cholesterol efflux in cell culture systems, no evidence has demonstrated that the peptides can indeed mimic apoA-I to form HDL particles. One of the peptides, D4F, synthesized with D-amino acids has been shown to reduce atherosclerosis in apoE-null mice (11, 12). In these studies, D4F increased pre-β HDL level. However, direct formation of HDL-like particles by D4F was not demonstrated. Moreover, in these studies HDL particles were identified using anti-apoA-I antibody for detection; there was no evidence that the 4F peptide was definitively within the HDL particles. One of the difficulties in demonstrating that these peptide mimetics directly form HDL particles is the lack of detection antibodies against these peptides. Although Wool et al. (13) and Meriwether et al. (14) attempted to use biotinylation of 4F peptide and [^{14}C]4F, respectively, to track the profile of peptide/lipoprotein association, no direct evidence is available to show that the peptide and apoA-I are in the same HDL particle.

In this study, we generated a peptibody by fusing 4F peptide to the Fc fragment of mouse IgG (mFc-2X4F). The rationale of using Fc is to generate a multivalent structure containing multiple amphipathic helices to examine whether multiple helices are superior for efflux compared with a monomeric helix. We also studied whether the peptibody is capable of forming HDL-like particle, inasmuch as apoA-I also contains multiple helices. Moreover, using an antibody against mouse Fc (mFc) as detection antibody, we were able to determine and track the size and distribution of HDL-like particles generated by mFc-2X4F in vitro and in vivo.

Manuscript received 29 September 2011 and in revised form 26 January 2012.

Published, JLR Papers in Press, January 27, 2012
DOI 10.1194/jlr.M020438

Abbreviations: CHD, coronary heart disease; FPLC, fast-protein liquid chromatography; HDL-C, HDL-cholesterol; IV, intravenous; LPDS, lipoprotein-deficient serum; PMA, phorbol 12-myristate 13-acetate.

[1] To whom correspondence should be addressed.
e-mail: slu@amgen.com

[S] The online version of this article (available at http://www.jlr.org) contains supplementary data in the form of two figures.

MATERIALS AND METHODS

Materials and cell culture

An ABCA1 antibody was obtained from Novus Biologicals (Littleton, CO), and apoA-I was obtained from Calbiochem (Rockland, MA). Lipoprotein-deficient serum (LPDS), phorbol 12-myristate 13-acetate (PMA), and TO901317 were purchased from Sigma (St. Louis, MO). All cells were obtained from American Type Culture Collection. HEK 293 cells were maintained in DMEM containing 10% FBS and penicillin/streptomycin. HEK 293 hABCA1 stable cell lines were generated in-house and maintained in DMEM containing 10% FBS and 400 μg/ml Geneticin. J774A.1 cells were maintained in DMEM containing 10% FBS and penicillin/streptomycin. HepG2 cells were maintained in MEM containing 10% FBS. THP1 monocytes were maintained in RPMI-1640 with 10% FBS and 0.5 mM 2-mercaptoethanol. THP1 monocytes were differentiated for 3–4 days in media containing 100 nM PMA. 3T3-L1 cells were cultured in high-glucose DMEM supplemented with 10% fetal calf serum and antibiotics. At confluence, adipocyte differentiation was initiated as described previously (15).

Animals

All mouse studies were conducted at Amgen, Inc. (Thousand Oaks, CA) and approved by the Institutional Animal Care and Use Committee. Male C57BL/6 mice were purchased from Charles River Laboratories (Frederick, MD). Mice were single-housed in a temperature-controlled environment with a 12 h light and 12 h dark cycle (06:30–18:30), and had free access to a standard chow diet (Harlan Teklad; Madison, WI) for at least 2 weeks before injection of the experimental materials. Compounds including apoA-I and mFc-2X4F were formulated in PBS in 100 μl volume at the indicated dose level. Mice were treated via intravenous (IV) injection, and blood samples were collected 4 h after each treatment.

Construction and purification

ApoA-I mimetic peptide 4F (Ac- DWFKAFYDKVAEKFKEAF-NH2) was custom-ordered from Midwest Biotech (Fishers, IN) and synthesized from L-amino acids. The mFc-4F (DWFKAFYDKVAEKFKEAF) and mFc-2X4F (DWFKAFYDKVAEKFKEAF-KVEPLRA-DWFKAFYDKVAEKFKEAF) (16) were constructed by fusing the peptides to the C-terminal end of mFc using overlapping oligonucleotides and PCR (17). The PCR fragment was inserted into the expression plasmid pAMG21, between the *Nde*I and *BamH*I sites. This plasmid was then transformed into *Escherichia coli* for expression. The expression of the peptibody was primarily in inclusion bodies. The protein was purified by protein A chromatography followed by ion exchange chromatography as described previously (18). All the purified material had endotoxin level <1EU/mg.

Cholesterol efflux assay

Cellular cholesterol was labeled with 1 μCi/ml [^{3}H]cholesterol (PerkinElmer Life Sciences; Waltham, MA) for 24 h in media supplemented with 1% LPDS. Cells were then washed twice and equilibrated for 18 h in media containing 0.2% FA-free BSA (Sigma). For J774A.1 cells, when indicated, ABCA1 level was induced with 0.3 mM 8-bromo-cAMP (Enzo; New York, NY). Cholesterol efflux was initiated with vehicle and various concentrations of apoA-I or peptide mimetics and incubated for 4 h. Cell media were collected and centrifuged at 3,000 rpm for 5 min to separate any cell debris. The cell monolayer was washed once with PBS and then lysed with 0.5 N NaOH. Cell media and cell lysates were transferred to individual scintillation vials and counted in a Beckman scintillation counter. Data were presented as percent cholesterol efflux.

ABCA1 stabilization in vitro

Cells were plated at 300,000 cells per well in 24-well cell culture dishes. THP1 cells were differentiated for 3 days with 100 nM PMA (Sigma). THP1 macrophages were treated for 18 h with 4 μM TO901317 (Sigma), and J774A.1 cells were treated with 0.3 mM 8-bromo-cAMP to boost ABCA1 expression. Cells were washed twice and then treated for 4 h (J774A.1) or 24 h (THP1) with vehicle, apoA-I, or mFc-2X4F at various concentrations. Following treatment, cells were washed with cold PBS and lysed with lysis buffer (30 mM Tris-HCl, 150 mM sodium chloride, 0.5 mM ethylenediaminetetraacetic acid, 10% glycerol, 1% NP-40, 0.5 mM PMSF, 1 mM sodium orthovanadate, 40 mM sodium fluoride, and protease inhibitor cocktail tablet). Lysates were collected and centrifuged at 13,000 rpm for 10 min at 4°C. Cleared lysates were normalized using the DC protein assay kit (Biorad; Hercules, CA). Western blots were analyzed using the Licor Odyssey imager.

Determination of plasma cholesterol level

Total cholesterol and HDL-cholesterol (HDL-C) were measured using an Olympus Analyzer (Olympus; Center Valley, PA). LDL-cholesterol was determined using a commercially available kit (Wako; Richmond, VA).

Measurement and analysis of HDL particles

The conditioned medium from ABCA1-expressing cells was fractionated by size-exclusion chromatography using a Superose 6 10/300 GL column (Amersham Biosciences; Piscataway, NJ) attached to a Beckman Gold System HPLC instrument. An online Beta-Ram Model 2 radiometric detector (IN/US Systems) was used to detect the [^{3}H]cholesterol. Mouse serum samples were fractionated by size-exclusion chromatography by incorporating two Superose 6 10/300 GL columns (Amersham Biosciences) in tandem, as described previously (19). Cholesterol, cholesteryl ester, and phospholipid contents were measured using the Colorimetric Cholesterol E Kit (Wako). The indicated fractions were run on 4–12% NuPAGE Bis-Tris gels (Invitrogen; Carlsbad, CA) and transferred onto nitrocellulose membrane (Invitrogen). ApoA-I was detected using an apoA-I antibody (Meridian Life Science; Saco, ME), and mFc-2X4F was detected using an anti-mouse Fc antibody (Sigma). For immunoprecipitation, the indicated mouse serum fractions were mixed with 5 μg apoA-I antibody (Meridian Life Science), apoB antibody (Abcam; Cambridge, MA), or anti-mouse Fc antibody (Sigma) and incubated overnight with gentle rotation at 4°C. Protein A and G agarose beads (Invitrogen) were then added to the samples and allowed to rotate for another 4 h. The immunoprecipitation complexes were then washed five times. Following the final wash, complexes were aspirated dry and prepared for Western blotting by adding Laemmli sample buffer (Biorad).

Two-dimensional nondenaturing gradient gel electrophoresis

ApoA-I-containing HDL subfractions were determined by two-dimensional nondenaturing gradient gel electrophoresis (2D-PAGE) as described previously (20, 21). Briefly, 5 μl of serum was separated by agarose (0.75%) gel electrophoresis in Tris-Tricine buffer (25 mM, pH 8.6) containing 3 mM calcium lactate at 4°C. Agarose gel strips were excised and annealed to 4–30% polyacrylamide gradient gels (CBS Scientific; Del Mar, CA) for separation in the second dimension. Electrophoresis was performed at 120 V for 24 h at 4°C in Tris-borate buffer (90 mM Tris, 80 mM boric

acid, and 2.5 mM EDTA). Separated lipoproteins were transferred to nitrocellulose membrane (0.45 μm; Invitrogen) at 50 V for 16 h at 4°C. The distribution of apoA-I-containing lipoproteins was detected with goat anti-mouse apoA-I antibody (Meridian Life Science) followed by rabbit anti-goat-HRP secondary antibody (Invitrogen). Mouse Fc was detected by goat anti-mouse mFc–HRP antibody (Santa Cruz Biotechnology; Santa Cruz, CA). Blots were visualized by enhanced chemiluminescence (Supersignal West Dura substrate; Thermo Scientific) by using an Alpha-Ease FC imager (Alpha Innotech; Santa Clara, CA). The intensity of the signal was quantified by densitometry.

Statistical analysis

Data analysis and EC_{50} values was estimated using Prism software (GraphPad Software, Inc.) All values are expressed as the mean ± SEM. Comparisons across groups were done using one-way ANOVA. When the ANOVA yielded a significant difference, post hoc analysis was done using Tukey's honestly significant difference test.

RESULTS

Structure of mFc-2X4F peptibody

Sequences and schematic presentation of 4F, mFc-4F, and mFc-2X4F are shown in **Fig. 1**. The molecular mass of full-length mFc-2X4F is about 62 kDa (dimer). When mFc-2X4F was run on reducing gel where the disulfide bonds between the Fc fragments were disrupted, the monomeric size was about 31 kDa. The sequence KVEPLRA was chosen as a linker to provide a flexible hinge domain as described previously. It was reported that the KVEPLRA fragment did not affect the efflux activity (16).

MFc-2X4F promoted cholesterol efflux in several cell lines

In this study, we first compared the efficacy and potency of reagents with different copy numbers of peptide helices in promoting cholesterol efflux. ApoA-I, 4F, mFc-4F, and mFc-2X4F had similar maximum efficiency in promoting cholesterol efflux in 293-ABCA1 recombinant cells. The potency of these molecules based on molar concentration units were in the order of apoA-I > mFc-2X4F > mFc-4F ≃ 4F (**Fig. 2A**). The EC_{50} value of mFc-2X4F is about 0.45 μM. When adjusted for the number of amphipathic helices, the order of potency did not change. The Fc fragment of the peptibody did not interfere with the efflux activity of the peptide. When the cells were treated with mFc fragment alone, no efflux activity was found (data not shown), indicating that the mFc part of peptibody was inert. The ability to remove cellular cholesterol by mFc-2X4F was ABCA1 dependent, because no efflux was observed in 293 parental cells using mFc-2X4F concentrations up to 3 μM (Fig. 2B, $P < 0.001$ vs. DMSO). To study whether the effects could also be observed in cells expressing endogenous ABCA1, mFc-2X4F was tested in J774A.1 and HepG2 cells. Interestingly, while apoA-I had greater ability to efflux cholesterol in J774A.1 cells, mFc-2X4F promoted efflux with higher efficiency than did apoA-I in HepG2 cells (Fig. 2C, D). In addition to macrophage and hepatoma cells, adipocytes have also been reported to efflux cholesterol. It has been shown that the ABCA1 gene is strongly induced upon differentiation of 3T3-L1 preadipocytes to mature fat cells and apoA-I promotes efflux in differentiated 3T3-L1 cells (15). Here we tested the ability of apoA-I, 4F, and mFc-2X4F in promoting efflux in differentiated 3T3-L1 cells. The mFc-2X4F-mediated efflux was at a level similar to that by apoA-I, but greatly exceeded 4F-mediated efflux (Fig. 2E, $P < 0.05$ vs. vehicle).

MFc-2X4F stabilized ABCA1 in vitro

ApoA-I has been shown to stabilize ABCA1 on the cell surface and to inhibit calpain-mediated proteolysis of ABCA1 (22). Consistent with previous findings, apoA-I dose-dependently stabilized ABCA1 in J774A.1 cells induced with 8-bromo-cAMP (**Fig. 3A**). MFc-2X4F exhibited a similar activity in stabilizing ABCA1 in J774A.1 cells in a dose-dependent manner (Fig. 3B). Both apoA-I and mFc-2X4F also stabilized ABCA1 protein levels to a similar degree in THP1 cells (Fig. 3C). These results indicate that mFc-2X4F may increase cholesterol efflux at least partly by stabilizing ABCA1 protein.

MFc-2X4F generated HDL-like particles in vitro

To characterize the nascent HDL particles generated by mFc-2X4F, 293-ABCA1 recombinant cells were loaded

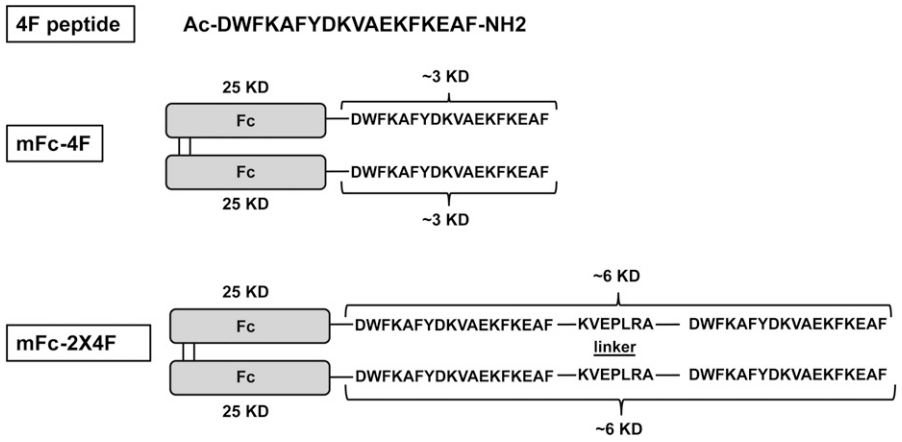

Fig. 1. Sequences and schematic presentation of 4F, mFc-4F, and mFc-2X4F.

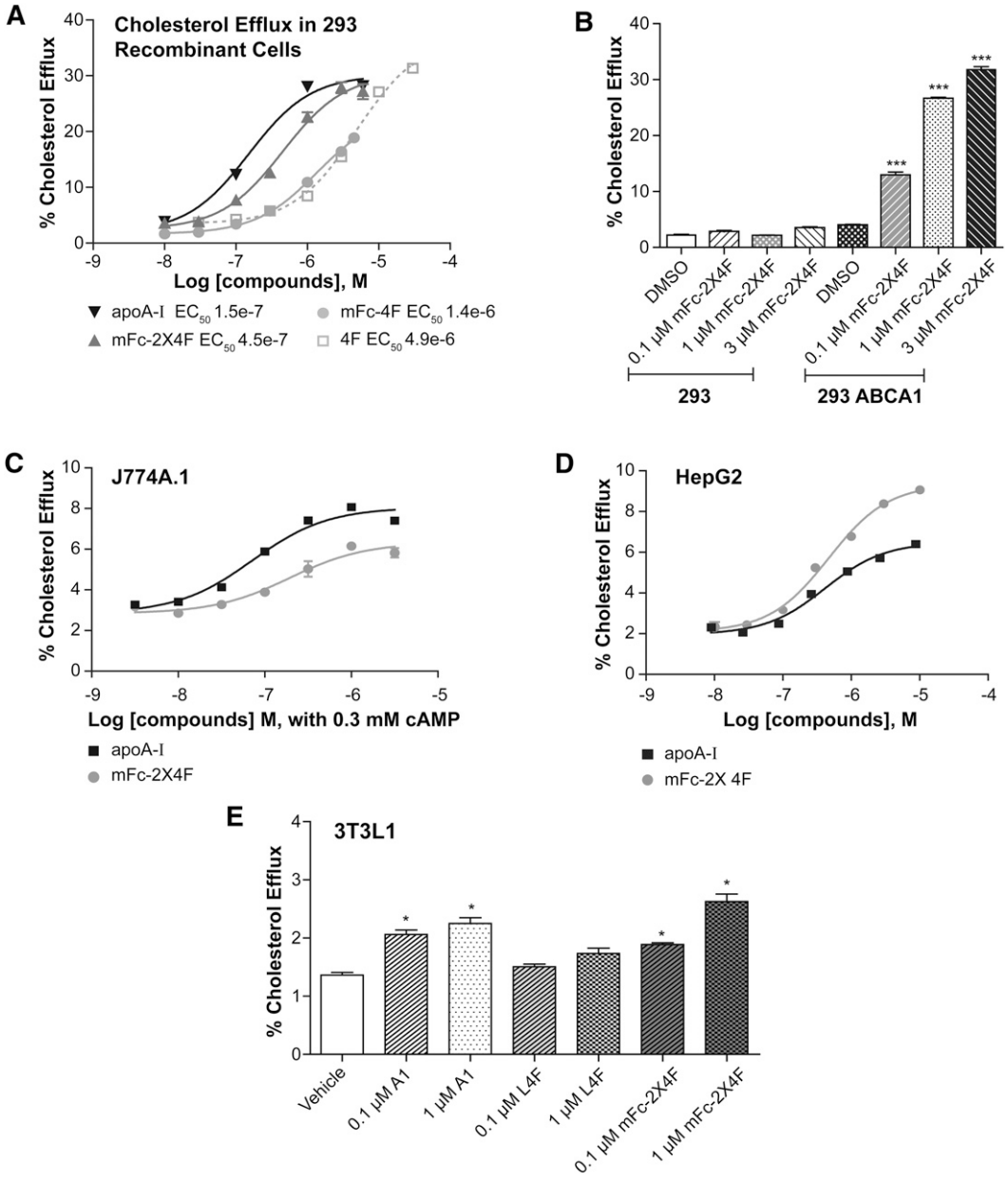

Fig. 2. Cholesterol efflux promoted by apoA-I and apoA-I mimetic peptides. A, B: 293 ABCA1 recombinant cells. C: J774A.1 macrophage cells. D: HepG2 hepatoma cells. E: 3T3-L1 cells. Cellular cholesterol was labeled with 1 μCi/ml [^{3}H]cholesterol for 24 h in media supplemented with 1% LPDS and equilibrated overnight before the treatment. J774A.1 was treated with cAMP to boost ABCA1 expression. Cells were treated with apoA-I or the indicated peptide mimetic for 4 h. The data are representative of three independent experiments with similar results. Data are expressed as mean ± SEM, n = 3 per group. *$P < 0.05$ compared with vehicle control; ***$P < 0.001$ compared with DMSO control.

with [^{3}H]cholesterol and treated with vehicle, apoA-I (1 μM) or mFc-2X4F (1 μM) for 4 h. The conditioned media containing nascent HDL were harvested and subjected to size-exclusion chromatography according to the protocol described above. Consistent with previous findings (23, 24), microparticles were formed by 293-ABCA1 recombinant cells (**Fig. 4A**). Large amounts of radiolabeled cholesterol were also released by the recombinant cells when treated with mFc-2X4F and apoA-I, respectively. The size of the nascent HDLs formed by mFc-2X4F was larger than those formed by apoA-I, based on the elution minutes on fast-protein liquid chromatography (FPLC). The size of the HDL particles correlated with the molecular mass of mFc-2X4F (62 kDa) and apoA-I (28 kDa). The peak fractions from mFc-2X4F or apoA-I were run on SDS-PAGE. Western blotting analysis using anti-apoA-I and anti-mouse Fc antibodies showed that the nascent HDL generated by apoA-I and mFc-2X4F consisted of the apolipoprotein and the peptibody mimetic, respectively (Fig. 4B). The results suggest that mFc-2X4F could mimic apoA-I not only to efflux cholesterol, but also to form HDL-like particles.

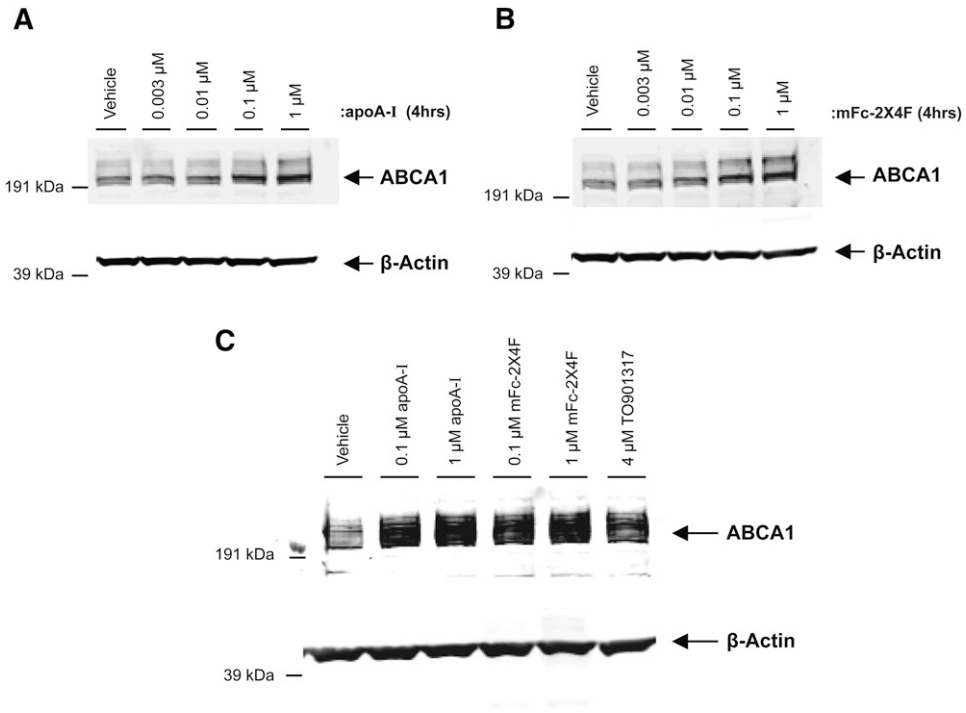

Fig. 3. ABCA1 stabilization by mFc-2X4F in J774A.1cells (A, B). C: THP1 cells. Differentiated THP1 macrophages were treated for 18 h with 4 μM TO901317, and J774A.1 cells were treated with 0.3 mM cAMP to boost ABCA1 expression. Cells were then treated for 4 (J774A.1) or 24 (THP1) h with vehicle (PBS), apoA-I, or mFc-2X4F at indicated concentrations.

MFc-2X4F generated HDL particles in vivo

To examine whether mFc-2X4F forms HDL particles in vivo, C57BL/6 mice were treated via IV injection with PBS, apoA-I (0.35 μmol/kg) or mFc-2X4F (0.35 μmol/kg). Blood samples were collected 4 h after the treatment, and plasma was prepared and analyzed for total, HDL, and LDL cholesterol. MFc-2X4F significantly increased total cholesterol level (**Fig. 5A**, $P < 0.01$). HDL-C showed a trend of increase when the animals were treated with mFc-2X4F (Fig. 5A, $P = 0.06$; PBS vs. mFc-2X4F). Although apoA-I treatment resulted in trends of increased total cholesterol and HDL-C, neither reached statistical significance (Fig. 5A). LDL-cholesterol levels were not significantly changed with all treatments (PBS: 15.29 ± 2.330 mg/dl; apoA-I: 24.54 ± 3.352 mg/dl; mFc-2X4F: 17.82 ± 1.928 mg/dl). Furthermore, the plasma samples were also fractionated using size-exclusion chromatography, and cholesterol levels were measured in each fraction using the Colorimetric Cholesterol E Kit (Wako). The major HDL peak from mFc-2X4F-treated animals was slightly shifted leftward, with a shoulder around fractions 51–58 when compared with PBS- and apoA-I-treated animals (Fig. 5B). This suggests that the HDL particles generated by mFc-2X4F are slightly larger in size (Fig. 5B). To determine the distribution of apoA-I and mFc-2X4F in the HDL fractions, the even-numbered fractions 36–70 covering LDL and HDL peaks were run on 4–12% SDS-PAGE and immunoblotted to detect apoA-I and mFc-2X4F, respectively (Fig. 5C). More apoA-I was detected in the HDL-containing fractions in the apoA-I- and mFc-2X4F-treated samples compared with PBS-treated samples (Fig. 5C). The majority of mFc-2X4F was located in particles larger than apoA-I (fractions 54–60) (Fig. 5C). It is noteworthy that the apoA-I-containing particles in the mFc-2X4F plasma shifted toward larger size compared with the apoA-I and PBS groups (Fig. 5C). Interestingly, these larger HDL particles also contain mFc-2X4F, suggesting that the formation of these particles may have involved both apoA-I and mFc-2X4F. Further, as the particle size increases in the samples from the mFc-2X4F-treated animals, there are still significant levels of mFc-2X4F, whereas the apoA-I level continues to diminish (Fig. 5C), suggesting that at least the formation of the large particles was mainly mediated by mFc-2X4F.

The phospholipid and cholesteryl ester levels were measured in HDL fractions. The area under the curve for phospholipid did not significantly vary between the mFc-2X4F- and PBS-treated samples (PBS: 90.36 ± 0.82 mg/dl; mFc-2X4F: 93.76 ± 1.04 mg/dl). Treatment with mFc-2X4F did not change cholesteryl ester levels when compared with PBS controls (PBS: 4.65 ± 0.23 mg/dl; mFc-2X4F: 5.03 ± 0.34 mg/dl).

MFc-2X4F treatment also increased particles that match the LDL size (Fig. 5B; fractions 36–52). All of these fractions contain mFc-2X4F and apoB (Fig. 5C and supplementary Fig. IA), whereas fractions 42–52 also contain small amounts of apoA-I. The apoB content in fractions 42–52 from mFc-2X4F-treated mice was similar to those from vehicle-treated mice. To determine whether apoB and mFc-2X4F coexist in the same particles, we immunoprecipitated apoB-containing fractions using an apoB antibody followed by Western blotting with an anti-mFc antibody.

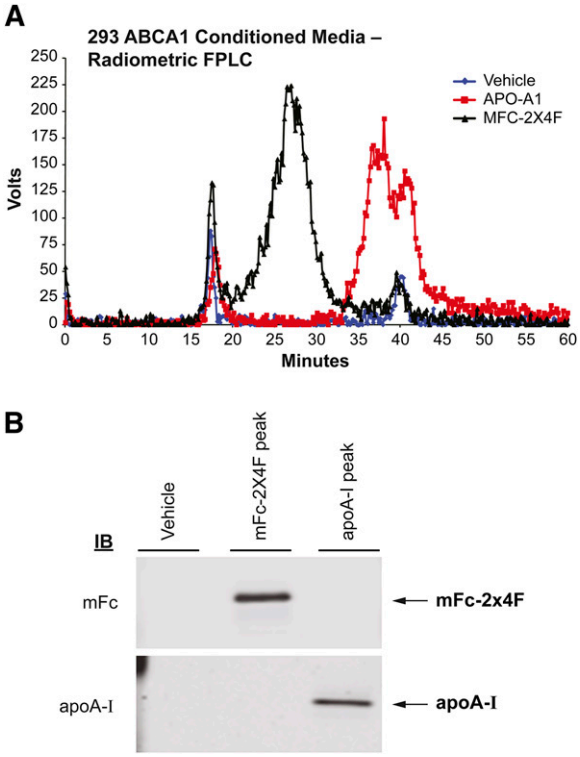

Fig. 4. Analysis of nascent HDL in 293-ABCA1 recombinant cells. A: FPLC elution profile of the conditioned media generated by apoA-I or mFc-2X4F in 293-ABCA1 recombinant cells. The 293-ABCA1 recombinant cells were treated with vehicle (PBS), apoA-I, or mFc-2X4F (1 μM) for 4 h. Media were collected from each treatment and concentrated 10-fold. Size-exclusion chromatography was performed using a Superose 6 10/300 GL column. An online Beta-Ram Model 2 radiometric detector (IN/US Systems) was used to detect the [^{3}H]cholesterol (1 V = 1,000 cpm). B: Western blot of the HDL peaks. The HDL peaks were collected, and 10 μl of each sample was run on SDS-PAGE and immunoblotted using antibody against apoA-I and mFc.

No mFc-2X4F was detected in the apoB-containing particles (see supplementary Fig. IB). The results suggest that the peak increase in fraction 36–39 does not represent LDL particles; rather, it is probably the larger HDL particles containing mFc-2X4F with a size similar to that of LDL particles.

MFc-2X4F and apoA-I coexisted in the same HDL particle

The distinct distribution of apoA-I and mFc-2X4F suggests that some apoA-I-containing particles could contain mFc-2X4F, whereas other particles may contain apoA-I devoid of the peptibody and vice versa. To further investigate whether mFc-2X4F and apoA-I coexist in the same particle, immunoprecipitation using anti-mouse apoA-I was performed with different fractions. Fraction 66 was selected for immunoprecipitation because it contained the highest level of apoA-I, whereas factions 54 and 56 were selected for mFc-2X4F content. Interestingly, apoA-I and mFc-2X4F were coimmunoprecipitated in all of the fractions we examined (**Fig. 6A**). Consistent with the data shown in Fig. 5C, fractions 54 and 56 had the highest levels of mFc-2X4F. There were two major bands representing mFc-2X4F; the lower band may be a clipped product of the full-length mFc-2X4F (~31 kDa). Immunoprecipitation using anti-mFc was also performed with the same fractions; however, neither apoA-I nor mFc-2X4F signal was found (data not shown). We believe that the Fc portion of mFc-2X4F could be sterically blocked or folded differently when bound to HDL, so that it is not accessible by the antibody. In summary, our data suggest that mFc-2X4F and apoA-I coexisted in the same HDL particle (Fig. 6B).

MFc-2X4F increased pre-β and α-1 HDL subfractions in vivo

To further investigate whether the distribution of the HDL subfractions was changed with mFc-2X4F treatment, plasma from PBS- and mFc-2X4F-treated mice was run on 2D-PAGE. Two identical sets of samples were run and then immunoblotted with apoA-I (**Fig. 7A**) and mFc (Fig. 7B) antibodies, respectively. Densitometry scanning was used for quantitative analysis for each subfraction. Treatment of mFc-2X4F significantly increased pre-β HDL by 75% and the large α-1 HDL particles by 100% (Fig. 7C). In contrast, the peptibody reduced α-3 HDL by about 25%. No significant change in α-2 HDL subfraction was observed. Interestingly, the majority of mFc-2X4F was located in the α-1 migrating HDL particles (Fig. 7B, right panel). The increase in large α-1 HDL particles was consistent with the result obtained using size-exclusion column where HDL-C peak was left-shifted (Fig. 5B).

DISCUSSION

In this study, we demonstrated that the apoA-I mimetic 4F peptibody, mFc-2X4F, is capable of mimicking apoA-I in promoting ABCA1-dependent cholesterol efflux, stabilizing ABCA1 protein and most importantly, forming HDL particles in vitro and in vivo. The 4F peptide has been shown to promote cholesterol efflux and to stabilize ABCA1 in the J774A.1 macrophage cell line (25). Here, we showed that the fusion of the N-terminus of 4F peptide to an Fc did not impair the activity of promoting cholesterol efflux and stabilizing ABCA1. On the contrary, the efflux activity was blunted when the C terminus of the peptide was fused to an Fc (data not shown). This result suggests that the C terminus of 4F peptide is important for interacting with the membrane. Furthermore, fusion of two tandem 4F peptides with an Fc fragment to form four helix complexes further increased the potency of promoting cholesterol efflux (Fig. 2). This result is consistent with previous studies showing that the number of helix repeats affects the ability of cholesterol efflux (16, 26, 27).

It is interesting to note that mFc-2X4F had different efficiency in promoting cholesterol efflux compared with apoA-I in different cell types. MFc-2X4F promoted efflux with higher efficiency than did apoA-I in HepG2 cells (Fig. 2D). HepG2 cells were found to secrete apoA-I naturally, and the secreted apoA-I promoted cholesterol efflux from the cells (28) in an autocrine fashion. The efflux measured in the mFc-2X4F-treated cells could represent the

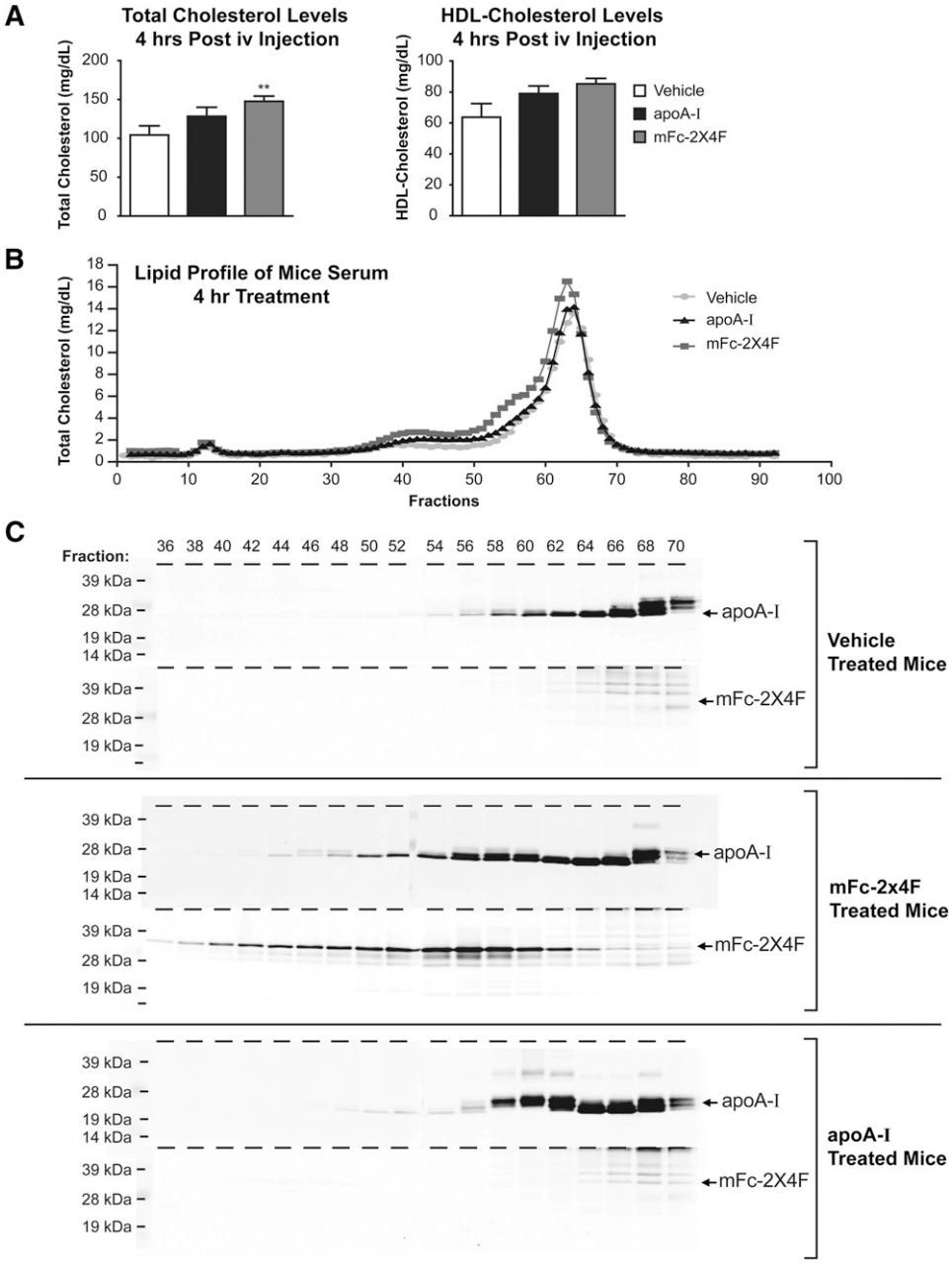

Fig. 5. Detection and analysis of HDL in C57BL/6 plasma. A: Total cholesterol and HDL level. C57BL/6 mice were IV injected with vehicle (PBS), apoA-I (0.35 μmol/kg), or mFc-2X4F (0.35 μmol/kg), and plasma was collected 4 h after injection. Total cholesterol and HDL-C were measured using the Olympus Analyzer. B: Lipid profile of plasma FPLC elutions. Plasma (100 μl) from individual mice was injected onto the column using an isocratic gradient of D-PBS containing 1.5 mM EDTA and 0.02% sodium azide. Fractions were collected on 0.5 ml V-bottom Costar 96-well plates, and cholesterol was measured using the Cholesterol E Kit (Wako). C: Distribution of apoA-I and mFc-2X4F. Even-numbered fractions 36–70 covering LDL and HDL peaks were run on 4–12% SDS-PAGE and immunoblotted for the presence of apoA-I and mFc-2X4F. Representative of n = 3 animals. Data are expressed as mean ± SEM. **P<0.01 versus vehicle group.

combined effects of the mimetic and the secreted apoA-I. Our results suggest that mFc-2X4F and apoA-I could have an additive effect in promoting cholesterol efflux in hepatocytes. This notion was also supported with the data obtained using 293-ABCA1 recombinant cells. The amount of cholesterol efflux from the cells was larger in the mFc-2X4F and apoA-I combination treatment than in the apoA-I alone (see supplementary Fig. II). The additive effects were more apparent at lower concentration of apoA-I, before cells reached their maximum capacity for efflux. These data suggest that apoA-I and mFc-2X4F may work cooperatively to efflux cholesterol.

One important finding in this study is that mFc-2X4F is capable of mimicking apoA-I to form nascent HDL particles in 293-ABCA1 recombinant cells. The FPLC elution profile of the medium from cells treated with the peptibody

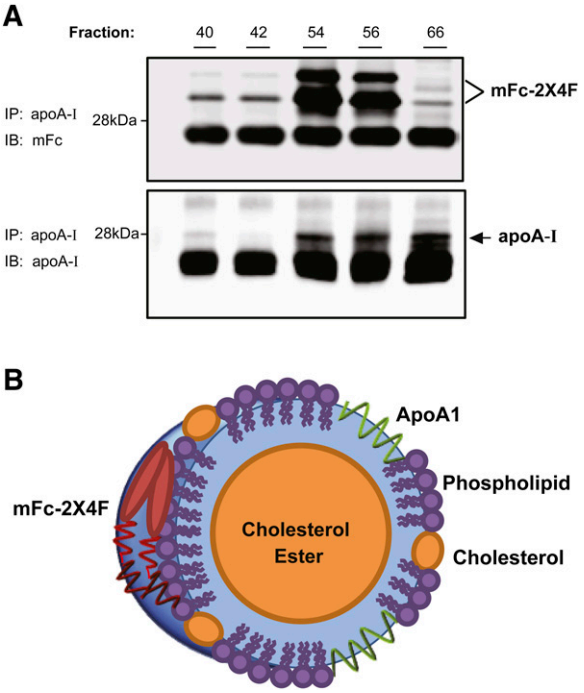

Fig. 6. ApoA-I and mFc-2X4F are colocated on HDL particles. A: Immunoprecipitation of HDL fractions. Indicated HDL fractions from Fig. 5 were immunoprecipitated using apoA-I antibody as described in Materials and Methods. The membrane was immunoblotted with anti-mFc antibody (top) and anti-apoA-I antibody (bottom). B: Schematic presentation of HDL particle generated by apoA-I and mFc-2X4F.

for 4 h was very similar to the apoA-I profile (Fig. 4A). The nascent HDL generated by mFc-2X4F eluted at earlier minutes indicates that the particles are larger in size compared with those generated by apoA-I. The difference in size reflects the molecular mass of mFc-2X4F, which is bigger than that of apoA-I. Most interestingly, we demonstrated that mFc-2X4F was present in the nascent HDL particles when analyzing the fractions using anti-mFc as a detection antibody. Duong et al. reported that the nascent HDL formed by apoA-I in J774A.1 macrophages contains two to four apoA-I molecules per particle (23). Studies using recombinant HDL particles reconstituted with POPC found that small discoidal HDL particles contained two antiparallel monomers of apoA-I (belt model) wrapped around a bilayer of phospholipids (29, 30). Larger HDL particles were also reported to contain up to four apoA-I molecules per particle (30). The nascent HDL particles formed by mFc-2X4F could also contain more than one molecule of mFc-2X4F per particle. When analyzing the HDL particles in mFc-2X4F-treated mice, we found that apoA-I and mFc-2X4F coexisted in the same HDL particles, and this could only be demonstrated when an anti-apoA-I antibody was used as the pull-down reagent, followed with an anti-Fc antibody for immunoblotting. However, when we used the Fc antibody as the pull-down reagent followed with an anti-apoA-I antibody for immunoblotting, we could not detect any band. These data suggest that the Fc part of the peptibody may have been sterically blocked and not available for detection. Further studies will need to be performed to analyze the lipid-bound conformation of the mFc-2X4F in the HDL particles.

We also measured the plasma cholesterol and lipoprotein distribution after the 4F peptibody treatment in mice (Fig. 5). Significant increases in plasma total cholesterol and lipoprotein-containing HDL were observed after treatment with 4F peptibody compared with PBS-treated controls. The major peak of the HDL from mFc-2X4F-treated animals was left-shifted when compared with PBS- and apoA-I-treated animals. Previous studies using 4F or D-4F (11, 13) reported no changes in total cholesterol levels and no apparent differences in the FPLC cholesterol trace after peptide treatment compared with PBS-treated mice. The most likely explanation for this difference is the efficacy in cholesterol efflux. Wool et al. reported that tandem peptides are better than 4F in their ability to promote efflux in a macrophage cell line (13). We showed in our study that mFc-2X4F has greater capability of promoting efflux compared with 4F in both 293-ABCA1 recombinant cells and differentiated 3T3-L1 cells. Our results suggest that the administration of mFc-2X4F may increase HDL-C by increasing the cholesterol efflux from peripheral cells and that mFc-2X4F may be superior to monomeric 4F peptide in terms of therapeutic potential.

One of our objectives, to design the 4F peptibody, was to address whether apoA-I and apoA-I peptide mimetic could coexist in the same HDL particles. Immunoblotting the fractions from FPLC with apoA-I and mFc antibody revealed that apoA-I and mFc-2X4F both appeared in the same fractions (Fig. 5C; fractions 44–64). Using immunoprecipitation experiments, we demonstrated that apoA-I and mFc-2X4F are present in the same HDL particle (Fig. 6). To our knowledge, this is the first direct evidence that apoA-I and peptide mimetic are colocated in the same cholesterol-rich particles. MFc-2X4F treatment also generated larger mFc-2X4F-containing HDL particles (fractions 36–39; Fig. 5C and supplementary Fig. IB). Taken together, there were at least two categories of HDL particles formed in the mFc-2X4F-treated mice: apoA-I- and mFc-2X4F-containing particles and mFc-2X4F-containing particles. The peptibody-containing HDL particles could be derived from the first step of cholesterol efflux in the peripheral tissues. This hypothesis is supported by the fact that mFc-2X4F is capable of forming HDL-like particles in 293-hABCA1 recombinant cells (Fig. 4). On the other hand, these particles could also be derived from the modification of preassembled HDL, because 4F peptide and 4F tandems have been shown to displace apoA-I from mouse HDL in vitro (16).

In addition to the increased pre-β HDL particles, plasma from mFc-2X4F-treated mice had higher large α-1 HDL but lower α-3 HDL (Fig. 7). Interestingly, mFc-2X4F was mostly present in the α-1 migrating particles. The shift in the distribution of HDL subfractions may be due to increased efficiency in HDL remodeling. HDL remodeling has been described as a mechanism for removal of lipid from atherosclerotic lesions (31). Patients with coronary heart disease (CHD) are reported to have lower

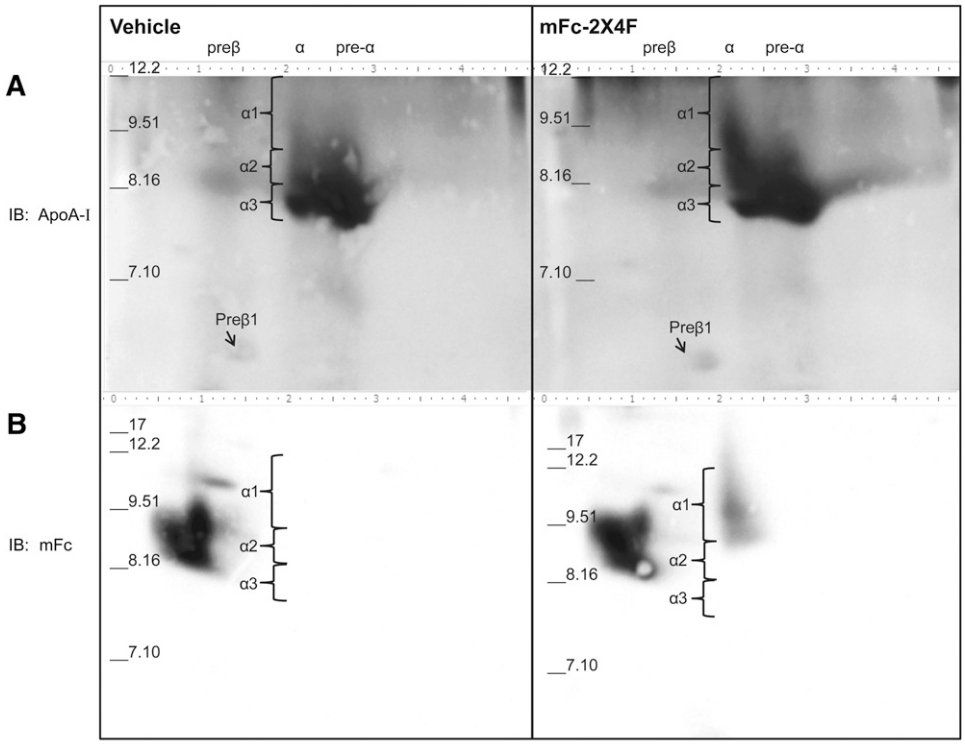

C

Fraction/ Intensity	Vehicle	mFc-2X4F	% Change
α-1	467235	927877	98%
α-2	478779	438249	-8%
α-3	639372	481197	-25%
Preβ1	28517	50114	75%

Fig. 7. MFc-2X4F increased pre-β HDL and α-1 HDL. Plasma was collected from C57BL/6 mice IV injected with vehicle (PBS, left panels) or mFc-2X4F (0.35 μmol/kg, right panels). 2D-PAGE was performed as outlined in Material and Methods. A: ApoA-I containing lipoproteins was detected with goat anti-mouse apoA-I antibody. B: MFc-2X4F was detected by goat anti-mouse IgG-HRP antibody. C: Densitometry of HDL subfractions. Representative 2D-PAGE and densitometry from one PBS- and one mFc-2X4F-treated sample was shown (n = 4 animals).

α-1 HDL, but higher α-3 HDL subfractions, compared with normal subjects (32). In both the Framingham Offspring and the Veterans Affairs HDL Intervention Trial, low levels of α-1 HDL were superior to total HDL-C levels in predicting CHD (33, 34). Moreover, treatment with niacin plus simvastatin significantly increased the large apoA-I-containing α-1 HDL particles, which appeared to be correlated with reduced coronary disease (35). Therefore, the mFc-2X4F-induced shift to larger HDL particles could have substantial therapeutic potential for the treatment of CHD.

In summary, we have demonstrated that mFc-2X4F promotes cholesterol efflux to form HDL-like particles from cells and generates peptibody-containing HDL particles in mice. In particular, it increases the α-1 HDL subfraction. Our results indicate that mFc-2X4F is a valuable tool molecule for studying HDL generated by the peptide mimetic. Further studies are needed to examine the therapeutic potential of this peptibody in treating atherosclerotic cardiovascular disease.

REFERENCES

1. Fielding, C. J., and P. E. Fielding. 1995. Molecular physiology of reverse cholesterol transport. *J. Lipid Res.* **36:** 211–228.
2. Rader, D. J., E. T. Alexander, G. L. Weibel, J. Billheimer, and G. H. Rothblat. 2009. The role of reverse cholesterol transport in animals and humans and relationship to atherosclerosis. *J. Lipid Res.* **50 (Suppl.):** 189–194.
3. Lawn, R. M., D. P. Wade, R. E. Hammer, G. Chiesa, J. G. Verstuyft, and E. M. Rubin. 1992. Atherogenesis in transgenic mice expressing human apolipoprotein(a). *Nature.* **360:** 670–672.
4. Pászty, C., N. Maeda, J. Verstuyft, and E. M. Rubin. 1994. Apolipoprotein AI transgene corrects apolipoprotein E deficiency-induced atherosclerosis in mice. *J. Clin. Invest.* **94:** 899–903.
5. Nissen, S. E., T. Tsunoda, E. M. Tuzcu, P. Schoenhagen, C. J. Cooper, M. Yasin, G. M. Eaton, M. A. Lauer, W. S. Sheldon, C. L. Grines, et al. 2003. Effect of recombinant ApoA-I Milano on coronary atherosclerosis in patients with acute coronary syndromes: a randomized controlled trial. *J. Am. Med. Assoc.* **290:** 2292–2300.
6. Segrest, J. P., R. L. Jackson, J. D. Morrisett, and A. M. Gotto, Jr. 1974. A molecular theory of lipid-protein interactions in the plasma lipoproteins. *FEBS Lett.* **38:** 247–258.
7. Segrest, J. P., H. De Loof, J. G. Dohlman, C. G. Brouillette, and G. M. Anantharamaiah. 1990. Amphipathic helix motif: classes and properties. *Proteins.* **8:** 103–117.

8. Segrest, J. P., M. K. Jones, H. De Loof, C. G. Brouillette, Y. V. Venkatachalapathi, and G. M. Anantharamaiah. 1992. The amphipathic helix in the exchangeable apolipoproteins: a review of secondary structure and function. *J. Lipid Res.* **33:** 141–166.
9. Anantharamaiah, G. M., J. L. Jones, C. G. Brouillette, C. F. Schmidt, B. H. Chung, T. A. Hughes, A. S. Bhown, and J. P. Segrest. 1985. Studies of synthetic peptide analogs of the amphipathic helix. Structure of complexes with dimyristoyl phosphatidylcholine. *J. Biol. Chem.* **260:** 10248–10255.
10. Navab, M., G. M. Anantharamaiah, S. T. Reddy, S. Hama, G. Hough, V. R. Grijalva, N. Yu, B. J. Ansell, G. Datta, D. W. Garber, et al. 2005. Apolipoprotein A-I mimetic peptides. *Arterioscler. Thromb. Vasc. Biol.* **25:** 1325–1331.
11. Navab, M., G. M. Anantharamaiah, S. Hama, D. W. Garber, M. Chaddha, G. Hough, R. Lallone, and A. M. Fogelman. 2002. Oral administration of an Apo A-I mimetic peptide synthesized from D-amino acids dramatically reduces atherosclerosis in mice independent of plasma cholesterol. *Circulation.* **105:** 290–292.
12. Navab, M., G. M. Anantharamaiah, S. T. Reddy, S. Hama, G. Hough, V. R. Grijalva, A. C. Wagner, J. S. Frank, G. Datta, D. Garber, et al. 2004. Oral D-4F causes formation of pre-beta high-density lipoprotein and improves high-density lipoprotein-mediated cholesterol efflux and reverse cholesterol transport from macrophages in apolipoprotein E-null mice. *Circulation.* **109:** 3215–3220.
13. Wool, G. D., T. Vaisar, C. A. Reardon, and G. S. Getz. 2009. An apoA-I mimetic peptide containing a proline residue has greater in vivo HDL binding and anti-inflammatory ability than the 4F peptide. *J. Lipid Res.* **50:** 1889–1900.
14. Meriwether, D., S. Imaizumi, V. Grijalva, G. Hough, L. Vakili, G. M. Anantharamaiah, R. Farias-Eisner, M. Navab, A. M. Fogelman, S. T. Reddy, et al. 2011. Enhancement by LDL of transfer of L-4F and oxidized lipids to HDL in C57BL/6J mice and human plasma. *J. Lipid Res.* **52:** 1795–1809.
15. Le Lay, S., C. Robichon, X. Le Liepvre, G. Dagher, P. Ferre, and I. Dugail. 2003. Regulation of ABCA1 expression and cholesterol efflux during adipose differentiation of 3T3-L1 cells. *J. Lipid Res.* **44:** 1499–1507.
16. Wool, G. D., C. A. Reardon, and G. S. Getz. 2008. Apolipoprotein A-I mimetic peptide helix number and helix linker influence potentially anti-atherogenic properties. *J. Lipid Res.* **49:** 1268–1283.
17. Latypov, R. F., T. S. Harvey, D. Liu, P. V. Bondarenko, T. Kohno, R. A. Fachini II, R. D. Rosenfeld, R. R. Ketchem, D. N. Brems, and A. A. Raibekas. 2007. Biophysical characterization of structural properties and folding of interleukin-1 receptor antagonist. *J. Mol. Biol.* **368:** 1187–1201.
18. Marston, F. A. 1986. The purification of eukaryotic polypeptides synthesized in Escherichia coli. *Biochem. J.* **240:** 1–12.
19. Garber, D. W., K. R. Kulkarni, and G. M. Anantharamaiah. 2000. A sensitive and convenient method for lipoprotein profile analysis of individual mouse plasma samples. *J. Lipid Res.* **41:** 1020–1026.
20. Asztalos, B. F., C. H. Sloop, L. Wong, and P. S. Roheim. 1993. Two-dimensional electrophoresis of plasma lipoproteins: recognition of new apo A-I-containing subpopulations. *Biochim. Biophys. Acta.* **1169:** 291–300.
21. Clay, M. A., and P. J. Barter. 1996. Formation of new HDL particles from lipid-free apolipoprotein A-I. *J. Lipid Res.* **37:** 1722–1732.
22. Wang, N., W. Chen, P. Linsel-Nitschke, L. O. Martinez, B. Agerholm-Larsen, D. L. Silver, and A. R. Tall. 2003. A PEST sequence in ABCA1 regulates degradation by calpain protease and stabilization of ABCA1 by apoA-I. *J. Clin. Invest.* **111:** 99–107.
23. Duong, P. T., H. L. Collins, M. Nickel, S. Lund-Katz, G. H. Rothblat, and M. C. Phillips. 2006. Characterization of nascent HDL particles and microparticles formed by ABCA1-mediated efflux of cellular lipids to apoA-I. *J. Lipid Res.* **47:** 832–843.
24. Nandi, S., L. Ma, M. Denis, J. Karwatsky, Z. Li, X. C. Jiang, and X. Zha. 2009. ABCA1-mediated cholesterol efflux generates microparticles in addition to HDL through processes governed by membrane rigidity. *J. Lipid Res.* **50:** 456–466.
25. Tang, C., A. M. Vaughan, G. M. Anantharamaiah, and J. F. Oram. 2006. Janus kinase 2 modulates the lipid-removing but not protein-stabilizing interactions of amphipathic helices with ABCA1. *J. Lipid Res.* **47:** 107–114.
26. Yancey, P. G., J. K. Bielicki, W. J. Johnson, S. Lund-Katz, M. N. Palgunachari, G. M. Anantharamaiah, J. P. Segrest, M. C. Phillips, and G. H. Rothblat. 1995. Efflux of cellular cholesterol and phospholipid to lipid-free apolipoproteins and class A amphipathic peptides. *Biochemistry.* **34:** 7955–7965.
27. Graversen, J. H., J. M. Laurberg, M. H. Andersen, E. Falk, J. Nieland, J. Christensen, M. Etzerodt, H. C. Thogersen, and S. K. Moestrup. 2008. Trimerization of apolipoprotein A-I retards plasma clearance and preserves antiatherosclerotic properties. *J. Cardiovasc. Pharmacol.* **51:** 170–177.
28. Chisholm, J. W., E. R. Burleson, G. S. Shelness, and J. S. Parks. 2002. ApoA-I secretion from HepG2 cells: evidence for the secretion of both lipid-poor apoA-I and intracellularly assembled nascent HDL. *J. Lipid Res.* **43:** 36–44.
29. Koppaka, V., L. Silvestro, J. A. Engler, C. G. Brouillette, and P. H. Axelsen. 1999. The structure of human lipoprotein A-I. Evidence for the "belt" model. *J. Biol. Chem.* **274:** 14541–14544.
30. Colvin, P. L., E. Moriguchi, P. H. Barrett, J. S. Parks, and L. L. Rudel. 1999. Small HDL particles containing two apoA-I molecules are precursors in vivo to medium and large HDL particles containing three and four apoA-I molecules in nonhuman primates. *J. Lipid Res.* **40:** 1782–1792.
31. Curtiss, L. K., D. T. Valenta, N. J. Hime, and K. A. Rye. 2006. What is so special about apolipoprotein AI in reverse cholesterol transport? *Arterioscler. Thromb. Vasc. Biol.* **26:** 12–19.
32. Asztalos, B. F., P. S. Roheim, R. L. Milani, M. Lefevre, J. R. McNamara, K. V. Horvath, and E. J. Schaefer. 2000. Distribution of ApoA-I-containing HDL subpopulations in patients with coronary heart disease. *Arterioscler. Thromb. Vasc. Biol.* **20:** 2670–2676.
33. Asztalos, B. F., L. A. Cupples, S. Demissie, K. V. Horvath, C. E. Cox, M. C. Batista, and E. J. Schaefer. 2004. High-density lipoprotein subpopulation profile and coronary heart disease prevalence in male participants of the Framingham Offspring Study. *Arterioscler. Thromb. Vasc. Biol.* **24:** 2181–2187.
34. Asztalos, B. F., D. Collins, L. A. Cupples, S. Demissie, K. V. Horvath, H. E. Bloomfield, S. J. Robins, and E. J. Schaefer. 2005. Value of high-density lipoprotein (HDL) subpopulations in predicting recurrent cardiovascular events in the Veterans Affairs HDL Intervention Trial. *Arterioscler. Thromb. Vasc. Biol.* **25:** 2185–2191.
35. Asztalos, B. F., M. Batista, K. V. Horvath, C. E. Cox, G. E. Dallal, J. S. Morse, G. B. Brown, and E. J. Schaefer. 2003. Change in alpha1 HDL concentration predicts progression in coronary artery stenosis. *Arterioscler. Thromb. Vasc. Biol.* **23:** 847–852.